Springer

Journal of
Mechanical
Science and
Technology

Journal of Mechanical Science and Technology 23 (2009) 3143~3152

www.springerlink.com/content/1738-494x
DOI 10.1007/s12206-009-0916-0

Maximizing structure performances of a sandwich panel with hybrid composite skins using particle swarm optimization algorithm †

Hee Keun Cho*

Senior researcher, Satellite Technology Research Center, Korea Advanced Institute of Science and Technology, Daejeon, Korea

(Manuscript Received September 24, 2008; Revised June 18, 2009; Accepted September 14, 2009)

Abstract

A sandwich panel, composed of hybrid laminate skins of AL (aluminum)-CFRP- GFRP and aluminum honeycomb core, was optimized for maximizing the structural performance. Stacking sequence of the three different materials comprising the hybrid laminate skins and individual ply angles are taken as design variables in the present optimization problem. Synergizing a particle swarm optimization (PSO) algorithm method with a specially developed FEM program enables one to optimally decide the design variables and thereby significantly improve the sandwich performance. The present technique applying PSO to a hybrid sandwich in conjunction with FEA has extended the application area of optimization with a complex honeycomb sandwich that is not possible by the conventional method.

Keywords: Composite material; Finite element analysis (FEA); Optimization; Sandwich

1. Introduction

Associated with their favorable response, sandwich structures have been utilized in widespread industrial areas. Depending on the specific requirements of the various applications, sandwich structures could have a wide variety of face and core materials. Moreover, a sandwich panel might need to be developed according to the necessities of required design criteria. Recently, in spacecraft application, the most general metal skins of the sandwich panel are prone to be replaced by laminate composite in order to overcome the limitation of a metal material. Motivated by this situation, and influenced by previous contributions [1-7], the present paper is directed at enhancing the structural performance of sandwich panels associated with SCF(stress concentration factor), stiffness, buckling, residual stress and failure by synergizing FEA and a PSO algorithm. Several researchers previously utilized a PSO to optimize structure optimization [8-10].

Unlike many conventional search gradient-based algorithms which move from one point to another along a gradient line in the design variable space, PSO algorithms work with a number of particles being based on a simplified social model that is closely tied to swarming theory and was first introduced by Kennedy and Eberhart (1995) [11]. Although the PSO algorithm has been applied to a wide range of engineering problems in the literature, few structural and, especially, hybrid laminate faced sandwich panel applications are known.

The objective of this work is to maximize the structural performance (i.e., stress concentration reduction, flexural stiffness, bend-twist stiffness, shear-extension stiffness, and buckling load) and minimize drawbacks (failure index and residual stresses) of sandwich panels which have hybrid laminate skins consisting of one aluminum ply, four CFRP-ply and four GFRP-ply by controlling respective ply angles and hybrid laminates' material stacking sequence. The solution approach combines two numerical analyses: (i) An FEA or a laminate computation is implemented to

† This paper was recommended for publication in revised form by Associate Editor Tae Hee Lee

*Corresponding author. Tel.: +82 42 350 8617, Fax.: +82 42 869 0064
E-mail address: marklee1@hanmail.net

obtain structure response at a certain ply layup and angle condition. (ii) The aforementioned PSO guides the objective function to the global extreme value by utilizing a random searching method.

2. Analytical formulation of laminated composite

2.1 Laminate analysis and finite element formulation [12-17]

A general laminate consists of an arbitrary number of layers. Formulating a simple working relationship between load, strain, and stress requires appropriate load-displacement relationships for the entire laminate. The lamination loads and moments are expressed in terms of the mid-surface strains $\{\varepsilon^0\}$ and curvature $\{\kappa\}$ as

$$\begin{Bmatrix} N_x \\ N_y \\ N_{xy} \\ M_x \\ M_y \\ M_{xy} \end{Bmatrix} = \begin{bmatrix} A_{11} & A_{12} & A_{16} & B_{11} & B_{12} & B_{16} \\ A_{12} & A_{22} & A_{26} & B_{12} & B_{22} & B_{26} \\ A_{16} & A_{26} & A_{66} & B_{16} & B_{26} & B_{66} \\ B_{11} & B_{12} & B_{16} & D_{11} & D_{12} & D_{16} \\ B_{12} & B_{22} & B_{26} & D_{12} & D_{22} & D_{26} \\ B_{16} & B_{26} & B_{66} & D_{16} & D_{26} & D_{66} \end{bmatrix} \begin{Bmatrix} \varepsilon_x^0 \\ \varepsilon_y^0 \\ \gamma_{xy}^0 \\ \kappa_x \\ \kappa_y \\ \kappa_{xy} \end{Bmatrix} \tag{1}$$

Each component of the $[A]$, $[B]$, and $[D]$ matrices is defined by

$$\begin{aligned} \left[A_{ij}\right] &= \sum_{k=1}^{N} \left[\bar{Q}_{ij}\right]_k (z_k - z_{k-1}) \\ \left[B_{ij}\right] &= \frac{1}{2}\sum_{k=1}^{N} \left[\bar{Q}_{ij}\right]_k \left(z_k^2 - z_{k-1}^2\right) \\ \left[D_{ij}\right] &= \frac{1}{3}\sum_{k=1}^{N} \left[\bar{Q}_{ij}\right]_k \left(z_k^3 - z_{k-1}^3\right) \end{aligned} \tag{2}$$

where $\bar{Q}_{ij}$ are the transformed reduced stiffnesses that are defined in terms of the material properties and orientation angles and z_k is the k th layer distance from the thickness center line. These matrices are termed: $\left[A_{ij}\right]$ is extensional matrix, $\left[B_{ij}\right]$ is extension-bending coupling matrix, $\left[D_{ij}\right]$ is bending stiffness matrix.

In the present investigation, the optimization is incorporated in a finite element analysis code. The potential energy, Π, of the plate can be expressed as

$$\Pi = \frac{1}{2}\int_A \bar{\varepsilon}^T \bar{\sigma} dA - \int_A \bar{u}^T p dA \tag{3}$$

where, p is the vector of in-plane mechanical loads. The plate is divided into a finite number of discretized elements. Element strain, $\bar{\varepsilon}$ can be written by using the displacement gradient matrix and nodal displacement vector, $\{d\}$ as

$$\bar{\varepsilon} = \left[B_0 + \frac{1}{2}B_L\right]\{d\} \tag{4}$$

where, B_0 and B_L are linear and non-linear strain-displacement matrices. Substituting for $\bar{\varepsilon}$ from Eq. (4) in Eq. (3) and then minimization of potential energy gives

$$\sum_{i=1}^{NE}\left(\left[K_0^e\right]\{d\} + \left[K_g^e\right]\{d\} - \{R\}\right) = 0 \tag{5}$$

where, NE is the number of elements. $\left[K_0^e\right]$ and $\left[K_g^e\right]$ are the linear and geometric element stiffness matrices and $\{R\}$ is the element load vector. These matrices are constructed using the procedure of reference 17 as, $\left[K_0^e\right] = \int_A B_0^T D B_0 \, dA$ $\left[K_g^e\right]\{d\} = \int_A B_L^T S \, dA$ and $\{R\} = \int_A H^T p \, dA$. Here S is the stress resultant matrix.

2.2 Objective functions for optimization

As mentioned in the previous sections, diverse aspects of the structural performance of sandwich panels are considered and optimized in the present study. The quality of optimization results of structures as well as other engineering problems highly depends on how to construct the objective function in the form of a distinctive equation. Therefore, the objective functions which have been implemented in optimization herein are established based on an analytical lamination theory and finite element formulations. The detailed categories and expressions are explained below.

2.2.1 Stress concentration factor

Stress concentration reduction in a perforated hybrid-sandwich is accomplished here by allowing the fiber orientation to vary locally. The plate is discre-

tized into 24 finite elements and the analysis reduces to finding the fiber direction in each element. This is achieved by mathematically interacting the PSO optimization algorithm with a finite element analysis. As shown in Fig. 2 the radius of the hole is equivalent to the half of a or b. The von Mises stress component was adopted in deciding SCF(stress concentration factor) and the object function can be written as follows.

$$f(\theta_i) = \sigma_e = \frac{1}{\sqrt{2}}\left[\left(\sigma_x - \sigma_y\right)^2 + \left(\sigma_x\right)^2 + \left(\sigma_y\right)^2 + 6\tau_{xy}^2\right]^{1/2} \quad (6)$$

where, θ_i is the ith element fiber angle of hybrid skin's material. The hybrid skins of orthotropic CFRP and GFRP were assumed to have the same fiber orientations consistently. The design variables controlled here are the only 24 individual elements' fiber angles, which can vary from -90 to 90 degrees continuously. The stacking sequence used as co-design variables in other optimization cases does not have meaning in this case so it had been omitted. Since the maximum stress occurs in the most stiff GFRP layer, its stresses are extracted for object function.

2.2.2 Flexural stiffness

Derivation procedure and mathematical representation of the flexural stiffness are similar to those of extensional stiffness. Accordingly flexural stiffness of a sandwich is a function of the skin's ply angle and overall thickness. As predicted, flexural stiffness is strongly dependent on the thickness and inversely proportional to h^3.

$$f(\theta_i, S_j) = \frac{12}{h^3}\left(w_1 \frac{D_{11}D_{22} - D_{12}^2}{D_{22}} + w_2 \frac{D_{11}D_{22} - D_{12}^2}{D_{11}}\right) \quad (7)$$

2.2.3 Buckling

Consider the calculation for the linearized buckling load for eigen buckling analysis. The stiffness matrices at time t and $t+\Delta t$ are ${}^tK$ and ${}^{t+\Delta t}K$, and the corresponding vectors of externally applied loads are ${}^tR$ and ${}^{t+\Delta t}R$. Linearized buckling analysis assumes that at any time, τ, the stiffness is ${}^\tau K = {}^tK + \lambda\left({}^{t+\Delta t}K - {}^tK\right)$ and external load is ${}^\tau R = {}^tR + \lambda\left({}^{t+\Delta t}R - {}^tR\right)$. Hence the objective function can be expressed as,

$$f(\theta_i, S_j) = \lambda = \frac{{}^\tau R - {}^t R}{{}^{t+\Delta t}R - {}^t R} \quad (8)$$

where λ (eigenvalues) is a buckling load scaling factor. If the initially applied load, ${}^tR$, is assumed to be zero, the final buckling load is λ times the applied external load, ${}^{t+\Delta t}R$, and the buckling load can be determined from the applied external load at time $t+\Delta t$.

2.2.4 Bend-twist coupling

The bending stiffness terms D_{16} and D_{26} couple the moment resultants M_x and M_y with the twisting curvature. The resulting effect is the tendency of the laminate to curl under applied uniform bending moments. Thus, the terms D_{16} and D_{26} are commonly referred to as the bending-twisting coupling terms.

$$f(\theta_i, S_j) = w_1 D_{16} + w_2 D_{26} \quad (9)$$

2.2.5 Shear-extension coupling

Similarly, the existence of the A_{16} and A_{26} terms in the in-plane stiffness matrix yields a coupling behavior termed shear-extension coupling. The net effect of these terms on the laminate response is the induction of shearing deformation under in-plane normal stress resultants N_x and N_y.

$$f(\theta_i, S_j) = w_1 A_{16} + w_2 A_{26} \quad (10)$$

2.2.6 Failure

The failure of composite structures is not as well understood, although numerous failure theories and models have been proposed. The Tsai-Wu criterion predicts failure when the failure index $\mathrm{F}I$ in a laminate reaches unity. For a single lamina in plane stress, $\mathrm{F}I$ is expressed as $\mathrm{F}I = F_1\bar{\sigma}_1 + F_2\bar{\sigma}_2 + F_{11}\bar{\sigma}_1^2 + F_{22}\bar{\sigma}_2^2 + F_{66}\bar{\sigma}_6^2 + 2F_{12}\bar{\sigma}_1\bar{\sigma}_2$ The aim of the optimization regarding laminate skin failure subjected to mechanical loading is to minimize the failure index $\mathrm{F}I$ in Eq. (11)

$$f(\theta_i, S_j) = \mathrm{F}I \quad (11)$$

The interaction term F_{12} is often approximated as $F_{12} = \bar{F}_{12}\sqrt{F_{11}F_{22}}$ with $-0.5 \le \bar{F}_{12} \le 0$. Each symbol's definition and more information of failure theory can be found in reference [15, 18]. The failure is examined at the center of all layers. The maximum

value of FI is minimized.

2.2.7 Residual stresses

It is important to distinguish the hygrothermal strains from the free expansion strains of the individual layers. The former includes the effect of the restraining action of the adjacent layers on one another as the laminate deforms as a whole. The latter ignores this constraining effect and represents the layer strains as if the layers are free to slide over one another. The difference between the hygrothermal strains at a given through the thickness location and the free expansion strains in that layer is the strain that causes stresses. Corresponding to these strains, one can calculate stresses induced by the constraining action of the neighboring layers. These hygrothermally induced residual stresses can be written as

$$\begin{Bmatrix} \sigma_x^R \\ \sigma_y^R \\ \tau_{xy}^R \end{Bmatrix} = \left[\bar{Q}_{ij}\right] \left(\begin{Bmatrix} \varepsilon_x^{0N} \\ \varepsilon_y^{0N} \\ \gamma_{xy}^{0N} \end{Bmatrix} + z \begin{Bmatrix} \kappa_x^N \\ \kappa_y^N \\ \kappa_{xy}^N \end{Bmatrix} - \begin{Bmatrix} \alpha_x \\ \alpha_y \\ \alpha_{xy} \end{Bmatrix} \Delta T + \begin{Bmatrix} \beta_x \\ \beta_y \\ \beta_{xy} \end{Bmatrix} \Delta C \right) \tag{12}$$

where α and β are thermal expansion coefficient and hygral coefficient, respectively. The objective function is the effective (von Mises) residual stress defined as

$$f(\theta_i, S_j) = \frac{1}{\sqrt{2}} \left[\begin{matrix} \left(\sigma_x^R - \sigma_y^R\right)^2 + \left(\sigma_x^R\right)^2 \\ + \left(\sigma_y^R\right)^2 + 6\left(\tau_{xy}^R\right)^2 \end{matrix} \right]^{1/2} \tag{13}$$

3. Particle swarm optimization

3.1 General comments

As discussed previously, the particle swarm optimization is applied here to a sandwich with hybrid laminate skins that could not be sufficiently optimized by gradient concept. The technique's basic scheme, whereby each particle keeps track of its coordinates in the problem space which are associated with the best solution it has achieved so far, is different from the gradient method by differential equation of objective function. The PSO's repeatedly updating the position of each particle over a time period to simulate the adaptation of the swarm to environment is highly effective since all of the multiple searching particles do not become trapped on a local convex or concave design space.

The position of each particle at each time step is updated by using the current position, a velocity vector, an inertia and a time increment. This process repeats until convergence [19]. The new position of each particle at iteration $k+1$ is obtained from

$$x_{k+1}^i = x_k^i + v_{k+1}^i \Delta t \tag{14}$$

where x_{k+1}^i is the position of particle i at iteration $k+1$, v_{k+1}^i is the corresponding velocity vector, and Δt is time step value. The velocity of each particle influences the incremental change in the position. Several different formulations for calculating velocity vector have been suggested. Kennedy and Eberhart(1995) [11] originally proposed the velocity vector formulation and Shi and Eberhart (1998) [20] later introduced an improved equation by involving an inertia term. The most widely used formulation in the literature is as follows:

$$v_{k+1}^i = w v_k^i + c_1 r_1 \frac{\left(p^i - x_k^i\right)}{\Delta t} + c_2 r_2 \frac{\left(p_k^g - x_k^i\right)}{\Delta t} \tag{15}$$

Here, p^i represents the best previous position of particle i so far, while p_k^g represents the global best position in the swarm. r_1 and r_2 are random numbers between 0 and 1. w is inertia term and two trust parameters, c_1 and c_2 are problem-dependent parameters. Typical PSO functions include problem parameters (inertia, trust), craziness, elite particle and velocity vectors [20].

3.2 Problem parameters

The inertia, w, in Eq. (15) is adjusted based on the coefficient of variation of the objective function to control searching scope parameters of the algorithm. With larger values they facilitate a more global behavior; if smaller, the tendency is the reverse. According to the literature of Shi and Eberhart the inertia range is $0.8 \le w \le 1.4$ and improved convergence rate was obtained when w is decreased linearly during the optimization. It dynamically changes during optimization to accelerate the convergence rate. In the current study w might vary from 1.2 at starting point to 0.9 at the end. c_1 is the trust parameter of

individual particles; on the other hand, c_2 is group's trust parameter. In the present study, constant values of $c_1 = 1.5$ and $c_2 = 2.5$ are used.

4. Application

The illustrative example of an AL-CFRP-GFRP hybrid laminate faced sandwich structure (a=1000 mm, b=600 mm for buckling; a=b=2r for stress concentration reduction in a perforated sandwich) is optimized with respect to the structural capabilities mentioned in the previous section 2.2, Fig. 1. Firstly, this study emphasizes reducing the tensile stress concentration factor in a uniaxially-loaded, central-circularly perforated hybrid sandwich by optimizing the fiber orientation locally throughout the layered hybrid skins. As far as the author knows, individual fiber orientation manipulation with PSO has never been introduced or tried in the literature until now.

For buckling performance optimization, the buckling load was obtained analytically with FEA. The model is divided, for convenience, into quadrilateral 60 discrete 3D, eight-node, isoparametric degenerated shell elements, respectively, of the type specially developed herein. Elements consist of nine-ply facesheet on both side and a honeycomb core, Fig. 1. The nine-ply facesheet laminate consists of one isotropic aluminum (6061 T6) ply (thickness=0.1 mm), four-ply orthotropic CFRP (T300/5208) with each 0.05 mm thick and again four-ply orthotropic GFRP (E-Glass/Epoxy) with the same thickness as the CFRP as shown in Fig. 1. Regarding the upper and lower bounds of the design variables, layer angle, θ_i, can change from -90 to 90 degrees with 15 degree interval; material stacking sequence variable, S_j, is able to select one of all possible six layup cases (the permutation of three different materials).

Motivated by Kennedy and Eberhart (1995) analysis [11], current analyses involve up to a population (particles) of 400 for making up a swarm. This is sufficient to prevent the analysis from termination at a local rather than global extreme value. Throughout all the optimizations performed in the present study, the sandwich panel is assumed to have symmetric layup against the mid-plane of the core and the respective elastic ply and core properties of Table 1 and 2. Additionally, one more constraint, same material plies should be stacked consecutively, is also given. The layer symmetry enables one to optimize just one side skin's components.

Table 1. Material properties of the hybrid laminate skin.

	CFRP (T300/5208)	GFRP (E-Glass/Epoxy)	AL (6061 T6)
E_{11} (GPa)	181.0	61.0	73.1
E_{22} (GPa)	10.3	24.8	
G_{12} (GPa)	7.2	12.0	27.5
υ_{12}	0.28	0.23	0.33
ρ (kg/m^3)	1600.	2100.	2700.
α_1, α_2 ($10^{-6}/{}^0C$)	0.02, 22.5	7.0, 21.0	23.8
β_1, β_2	0, 0.6	0, 0.2	-
X (MPa)	2303	1080	276
X' (MPa)	951	128	
Y (MPa)	35	39	
Y' (MPa)	250	128	
S (MPa)	80	89	

Table 2. Material properties of the aluminum honeycomb core.

	Al honeycomb core
$E_x = E_y$ (GPa)	≈ 0
E_z (GPa)	1.0
G_{xy} (GPa)	≈ 0
G_{xz} (GPa)	0.44
G_{yz} (GPa)	0.22
υ_{xy}	0.8
$\upsilon_{yz} = \upsilon_{xz}$	≈ 0
ρ (kg/m^3)	16.
α ($10^{-6}/{}^0C$)	23.8

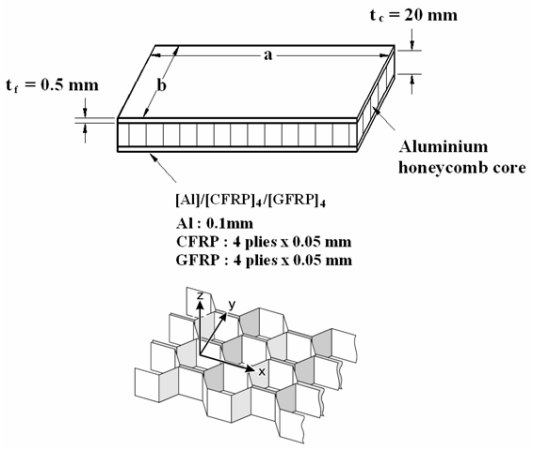

Fig. 1. Hybrid laminate (AL/CFRP/GFRP) faced honeycomb sandwich panel.

The purpose of this analysis is to maximize extensional stiffness, flexural stiffness, buckling load, bend-twist coupling stiffness, shear-extension coupling stiffness and minimize failure index and residual stresses of the illustrated sandwich panel by controlling stacking sequence of three different materials (AL, CFRP, GFRP) and ply angles of the respective orthotropic layers. Optimization analyses for those characteristics were implemented independently and best layup sequences and corresponding ply angles were obtained. The system searches for the optimum values of objective functions using the previously described PSO algorithm. The objective function, $f(\theta_i, S_j)$, is defined in equations (6) to (13).

The two kinds of interdependent design variables that increase the complexity in searching solution are manipulated simultaneously in PSO. Isotropic and composite ply properties used are representative of aluminum (6061 T6), unidirectional graphite epoxy (T300/5208) and E-glass epoxy with uniform fiber content/spacing throughout.

Fig. 1 and Tables 1 and 2 include the dimensions and material properties. Individual composite plies are assumed to be transversely isotropic with hexagonal packing. The core is 20 mm thick, whereas the skin is 0.5 mm thick. Optimization begins with initial stacking sequence AL-CFRP-GFRP, all zero layer angles and zero individual element fiber angles.

5. Results

Several physical properties of a hybrid laminate faced sandwich panel of Fig. 1 and perforated uniaxially loaded sandwich plate were optimized in the present study. The objective functions, a measure of the performance, were maximized by simultaneously controlling locally fiber direction or layer direction and/or material stacking sequence of isotropic-orthotropic ply mixed hybrid laminate skins. This paper extends the application bounds of sandwich optimization by utilizing non-gradient optimization algorithm PSO in conjunction with FEA.

Ability to enhance the mechanical performance of fibrous composite sandwich panels by optimally setting up the skin plies taking advantage of graphical method is described in the literature [13, 21].

Unlike here, Ref. [13, 21] restricts the composite facesheet only to have uniform plies (i.e., single composite material) and symmetric-balanced layups. Virtually nothing appears to be available in the literature regarding handling a hybrid laminate skin with arbitrary stacking sequence. Most previous studies emphasize changing the stacking sequence of rectilinear plies or layer thickness. The alternate approach described here adjusts both locally fiber angle or ply angle and material stacking sequence at the same time to make the sandwich have the best capability with respect to the presented hybrid sandwich panel using the PSO algorithm.

The results of seven optimization cases in section 2.2, i.e., minimizing or maximizing of physical properties of composite sandwich analyzed: (i) stress concentration factor, (ii) flexural stiffness, (iii) buckling load, (iv) bend-twist coupling stiffness, (v) shear-extension coupling stiffness, (vi) failure index and (vii) residual stress are presented in Figs. 3 through 5 and Table 3. Fig. 2 illustrates (a) the geometry and b.c, (b) initial fiber direction aligned horizontally and (c) final optimized layout. The fiber orientation is constant within each element, but it can change from element-to-element. This optimum design approach presented exhibits better performance than previous design and the synergized numerical optimization procedure is highly effective. The SCF has been drastically decreased from 11.2 to 4.2 by means of locally handling fiber direction with PSO. About 62% of the initial maximum stress has been decreased.

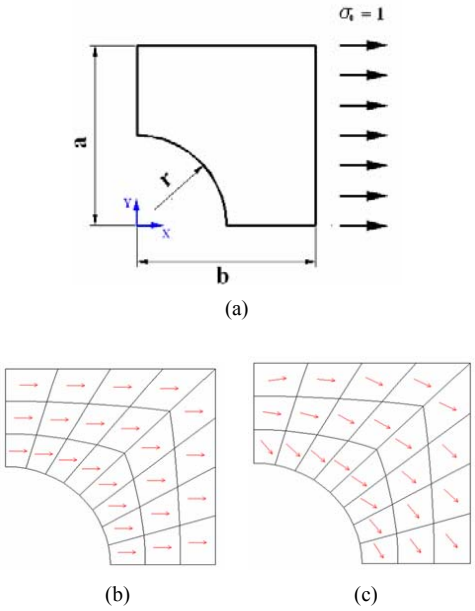

Fig. 2. Locally fiber direction optimization in order to minimize S.C.F (stress concentration factor): (a) geometry and b.c., (b) initial fiber direction, (c) optimized fiber direction.

Table 3. Optimized layup angles and material stacking sequences of the hybrid laminate faced sandwich with PSO.

Optimized layer angle and material stacking sequence			Objective value(f)		
			(Initial)	(First)	(Final)
Stress concentration factor (min.)			(SCF)		
Fig. 2			11.2	8.7	4.2
GFRP	CFRP				
Flexural stiffness (max.)			(MPa)		
-	90/0/0/90	0/90/0/90	8601.6	9413.0	9854.9
AL	CFRP	GFRP			
Buckling load (max.)			(MPa)		
90/90/90/0	-	0/90/90/90	3762.6	6769.1	6962.5
CFRP	AL	GFRP			
Bend-twist coupling stiffness (max.)			(N·mm)		
-45/-45/-45/-45	-45/-45/-45/-45	-	7.1e5	1.8e6	2.2e6
CFRP	GFRP	AL			
Shear-extension coupling stiffness (max.)			(N/mm)		
45/45/45/45	45/45/45/45	-	7.5e3	1.4e4	2.1e4
GFRP	CFRP	AL			
Failure index (min.)			-		
45/-45/-45/45	-	-45/-45/45/45	27.4	10.87	7.1
CFRP	AL	GFRP			
Residual stress (min.)			(MPa)		
90/90/90/90	90/90/90/90	-	305.9	280.1	185.7
GFRP	CFRP	AL			

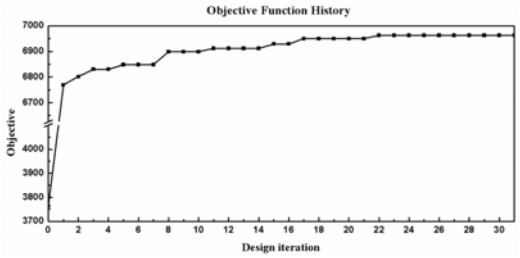

(a) Buckling load

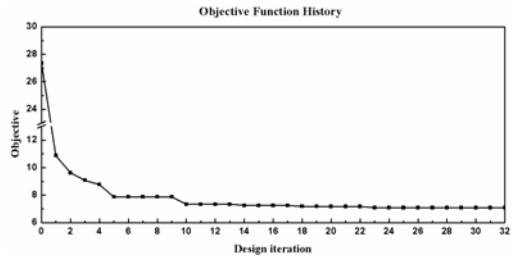

(b) Failure index

Fig. 3. Change in buckling load (a), and failure index, (b), in optimized sandwich plate with number of iterations.

The other respective evaluated final objective values for the sandwich by PSO are 9854.9, 6962.5, 2.2e6, 2.1e4, 7.1 and 185.7 (Table 3). Compared with the initial (random) layup hybrid sandwich, the structural performance enhances 47.8% for the extensional stiffness, 14.6% (flexural stiffness), 85.0% (buckling load), 209.8% (bend-twist coupling stiffness), 186.7% (shear-extension coupling stiffness), 74.1% (failure index) and 39.3% (residual stress). Furthermore, it should be noted that since relative large population size, 400, was used, drastic improvement of objective function after first iteration, mid-column data of Table 3 objective value, was achieved. This shows that the population size of 400 is good enough for this problem.

Additionally, shear force $N_{xy} = 200\,N/mm$ and twisting moment $M_{xy} = 100\,N \cdot mm/mm$ acting on the sandwich are given for failure analysis. A number of external and/or internal effects give rise to residual stresses. However, hygrothermally-induced residual stress [22] is herein only considered. The residual stress of sandwich skin subjected to temperature

increase ΔT =200℃ and 2.0% moisture change with reference 0% is minimized by controlling design variables which are defined previously.

Table 3 compares the value of material stacking sequence and corresponding layer angles for the optimized nine-ply AL-CFRP-GFRP laminate with each other. The result of buckling optimization in Table 3, CFRP(90/90/90/0)-AL-GFRP(0/90/90/90), agrees well with the knowledge that in general for buckling phenomena, the farther the location of the most stiffness material from the center line, the greater buckling resistance that can be obtained.

On the other hand, the material stacking order is reversed, GFRP-AL-CFRP, in residual stress analysis. Both humidity and temperature interaction results in increasing the complexity of stress distribution. The middle isotropic aluminum ply intervenes between two different materials regarding directional hygrothermal expansion rates, i.e., GFRP's 1-directional thermal expansion coefficient is 7 whereas that of CFRP is nearly 0. The minimum failure index, Eq. (11), for the optimized hybrid sandwich skin by PSO of 7.1 represents a 74.1% reduction in failure index compared with 27.4 for the initial random hybrid laminate (Table 3). Such a failure index reduction is significant since a structure's strength, and therefore its design and ultimately its weight, can depend on failure index. In all analysis cases, the initial objective values were achieved by using the randomly selected design variables.

Fig. 3 demonstrates how the present object function and design variables for the optimization of both buckling load, Eq. (8), and failure index, Eq. (11), extremized to the optimum value with increased number of iterations. The present PSO is well suited for the current problem in that all material stacking order and ply angles are stored in a particle and the process (design) moves toward a global optimum based on the social model that is closely tied to swarming theory. The analyses satisfied the convergence criteria (absolute and relative objective and design variable convergence) at 31st (buckling) and 32nd (failure) iteration with 400 particles, which is fairly extensive.

Figs. 4 and 5 illustrate the history of the variation of the ply angles and the case number of the skin material stacking order as obtained from the elite particles. The high initial fluctuations indicate objective values have not fully stabilized at the beginning of the PSO.

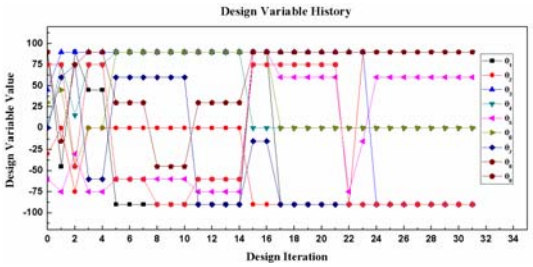

(a) Maximizing buckling load

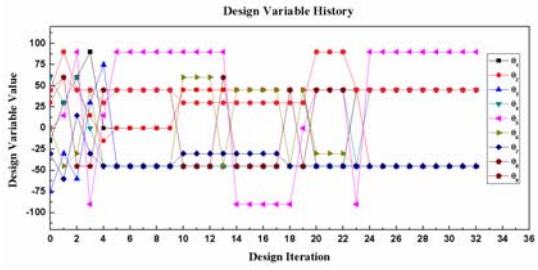

(b) Minimizing failure index

Fig. 4. Variation of the ply angles ($\theta_1 \sim \theta_9$) in buckling load, (a), and failure index, (b), optimization.

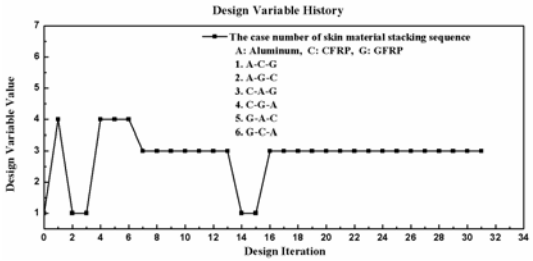

(a) Maximizing buckling load

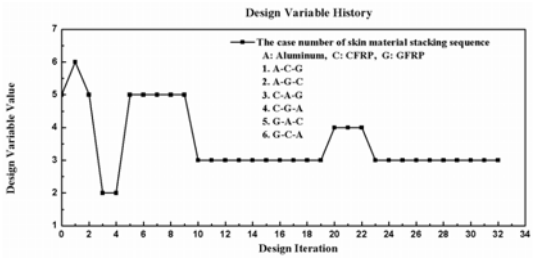

(b) Minimizing failure index

Fig. 5. Variation of the number of material stacking sequence case (S_1) in buckling load, (a), and failure index, (b), optimization.

6. Conclusion

Optimal design of sandwich panels with hybrid AL-CFRP-GFRP skins and aluminum honeycomb cores with respect to seven physical performances in section 2.2 is obtained by the use of the non-gradient optimization algorithm PSO described in the paper. An optimization scheme, which synergizes a PSO and FEA, enables one to drastically enhance the structure performance of the practical sandwich panels with hybrid laminate skins. Most previous optimization studies of general sandwich structure tend to emphasize aspects such as modifying simple core and/or isotropic-skin thickness, cost, weight, stiffness of balanced symmetric skin through the plate. The present extension to arbitrary hybrid laminate-faced honeycomb sandwich panel overcomes limitations of previous studies, thereby extending the applicability. The introduced technique involves simultaneously controlling individual (element fiber directions) or interdependent (material stacking sequence and ply angles of skin) design variables by synergizing a PSO algorithm and FEA. The method therefore provides more than just a suitable stacking sequence of various rectilinearly uniform orthotropic plies. The author is unaware of previously published results which control ply angle and hybrid laminate stacking sequence of sandwich skin at the same time.

The present employment of PSO is less likely than gradient methods to become trapped in local solutions. Rather, they progress to a global optimum solution. This advantage of PSOs, plus their ability to accurately satisfy an objective function, guarantees reliable solutions of complicated engineering problems like that analyzed here.

Acknowledgment

The author wishes to acknowledge the support of the Satellite Technology Research Center of KAIST project STSAT-3.

References

[1] B. Malott, R. C. Averill, E. D. Goodman, Y. Ding and W. F. Punch, Use of genetic algorithms for optimal design of laminated composite sandwich panels with bending-twisting coupling, *Proc. of the 37th AIAA/ASME/ASCE/AHS Structures, Structural Dynamics and Materials*, Salt Lake City, USA. (1996).

[2] M. Walker and R. Smith, A computational methodology to select the best material combinations and optimally design composite sandwich panels for minimum cost, *Computers and Structures*, 80 (2002) 1457-60.

[3] J. C. M. Theulen and A. A. J. M. Peijs, Optimization of the bending stiffness and strength of composite sandwich panels, *Composite Structures*, 17 (1) (1991) 87-92.

[4] A. Muc and P. Zuchara, Buckling and failure analysis of FRP faced sandwich plates, *Composite Structures*, 48 (1) (2000) 145-150.

[5] G. C. Saha, A. L. Kalamkarov and A. V. Georgiades, Effective elastic characteristics of honeycomb sandwich composite shells made of generally orthotropic materials*, Compos Part A*, 38 (6) (2007) 1533-1546.

[6] Y. M. Kong, S. H. Choi, B. S. Yang and B. K. Choi, Development of integrated evolutionary optimization algorithm and its application to optimum design of ship structures, *Journal of Mechanical Science and Technology*, 22 (2008) 1313-1322.

[7] A. Samad and K. Y. Kim, Multi-objective optimization of an axial compressor blade, *Journal of Mechanical Science and Technology*, 22 (2008) 999-1007.

[8] G. Venter and J. Sobieszczanski-Sobieski, Multidisciplinary optimization of a transport aircraft wing using particle swarm optimization, *Structural and Multidisciplinary Optimization*, 26 (1) (2004) 121-31.

[9] P. C. Fourie and A. A. Groenwold, The particle swarm optimization algorithm in size and shape optimization, *Structural and Multidisciplinary Optimization*, 23 (2002) 259-67.

[10] P. C. Fourie and A. A. Groenwold, Particle swarms in topology optimization, *4th world congress of structural and multidisciplinary optimization*, China, (2001) 52.

[11] J. Kennedy and R. Eberhart, Particle swarm optimization, *Proceedings of IEEE international conference on neural networks*, Perth Australia, (1995) 1942.

[12] R. Spallino and S. Rizzo, Optimal design of laminated composite plates, *Computer Aided Optimum Design of Structures*, 40 (1999) 277-286.

[13] Z. Gürdal, R. T. Haftka and P. Hajela, *Design and Optimization of Laminated Composite Materials*, Wiley-Interscience Publication, New York, USA,

(1998).

[14] J. R. Vinson, *The Behavior of Sandwich Structures of Isotropic and Composite Materials*, Technomic Publishers, New York, USA, (1999).

[15] G. H. Staab, *Laminar Composites*, Butterworth Heinemann, Boston, USA, (1999).

[16] K. J. Bathe, *Finite Element Procedures in Engineering Analysis*, Prentice-Hall, NJ, USA, (1982).

[17] O. C. Zienkiewicz and R. L. Taylor, *The Finite Element Method*, Butterworth Heinemann, Boston, USA, (2005).

[18] A. A. Groenwold and R. T. Haftka, Optimization with non-homogeneous failure criteria like Tsai-Wu for composite laminates, *Structural and Multidisciplinary Optimization*, 32 (3) (2006) 183-190.

[19] I. C. Trelea, The particle swarm optimization algorithm: convergence analysis and parameter selection, *Information Processing Letters*, 85 (6) (2003) 317-325.

[20] Y. H. Shi and R. C. Eberhart, A modified particle swarm optimizer, *Proc. of IEEE International Conference of Evolutionary Computation*, Anchorage, USA, (1998).

[21] M. Miki, K. Fujimori and Y. Miyano, Optimal design of fibrous composite sandwich plates with required flexural stiffness, *JSME International Journal*, 33 (364) (1983) 49-54.

[22] N. V. Swamy Haidu and P. K. Sinha, Nonlinear transient analysis of laminated composite shells in hygrothermal environments, *Composite Structures*, 72 (3) 2006) 280-288.

Hee Keun Cho, who received his Ph. D. in Mechanical Engineering from University of Wisconsin-Madison, WI, USA, in 2006, has over 40 publications in theoretical & numerical analysis; composite, finite element analysis, optimization, functionally graded materials. Dr. Cho is currently working at Satellite Technology Research Center of KAIST and involved in the Satellite Development Project (STSAT-3) administrated by the government.